TU Delft

Delft University of Technology

Patient-derived organoids can predict response to chemotherapy in metastatic colorectal cancer patients

Ooft, Salo N.; Weeber, Fleur; Dijkstra, Krijn K.; McLean, Chelsea M.; Kaing, Sovann; van Werkhoven, Erik; Schipper, Luuk; Hoes, Louisa; Wessels, Lodewyk; More Authors

DOI
10.1126/scitranslmed.aay2574

Publication date
2019

Document Version
Final published version

Published in
Science Translational Medicine

Citation (APA)
Ooft, S. N., Weeber, F., Dijkstra, K. K., McLean, C. M., Kaing, S., van Werkhoven, E., Schipper, L., Hoes, L., Wessels, L., & More Authors (2019). Patient-derived organoids can predict response to chemotherapy in metastatic colorectal cancer patients. *Science Translational Medicine*, *11*(513). https://doi.org/10.1126/scitranslmed.aay2574

Important note
To cite this publication, please use the final published version (if applicable).
Please check the document version above.

Copyright
Other than for strictly personal use, it is not permitted to download, forward or distribute the text or part of it, without the consent of the author(s) and/or copyright holder(s), unless the work is under an open content license such as Creative Commons.

Takedown policy
Please contact us and provide details if you believe this document breaches copyrights.
We will remove access to the work immediately and investigate your claim.

This work is downloaded from Delft University of Technology.
For technical reasons the number of authors shown on this cover page is limited to a maximum of 10.

CANCER

Copyright © 2019 The Authors, some rights reserved; exclusive licensee American Association for the Advancement of Science. No claim to original U.S. Government Works

Patient-derived organoids can predict response to chemotherapy in metastatic colorectal cancer patients

Salo N. Ooft[1,2]*, Fleur Weeber[1,2]*, Krijn K. Dijkstra[1,2†], Chelsea M. McLean[1,2†], Sovann Kaing[1,2], Erik van Werkhoven[3], Luuk Schipper[1,2], Louisa Hoes[1,2], Daniel J. Vis[2,4], Joris van de Haar[1,2,4], Warner Prevoo[5], Petur Snaebjornsson[6], Daphne van der Velden[1,2‡], Michelle Klein[1,2], Myriam Chalabi[1], Henk Boot[7], Monique van Leerdam[7], Haiko J. Bloemendal[8], Laurens V. Beerepoot[9], Lodewyk Wessels[2,4,10], Edwin Cuppen[2,11,12], Hans Clevers[2,13,14], Emile E. Voest[1,2,7§]

There is a clear and unmet clinical need for biomarkers to predict responsiveness to chemotherapy for cancer. We developed an in vitro test based on patient-derived tumor organoids (PDOs) from metastatic lesions to identify nonresponders to standard-of-care chemotherapy in colorectal cancer (CRC). In a prospective clinical study, we show the feasibility of generating and testing PDOs for evaluation of sensitivity to chemotherapy. Our PDO test predicted response of the biopsied lesion in more than 80% of patients treated with irinotecan-based therapies without misclassifying patients who would have benefited from treatment. This correlation was specific to irinotecan-based chemotherapy, however, and the PDOs failed to predict outcome for treatment with 5-fluorouracil plus oxaliplatin. Our data suggest that PDOs could be used to prevent cancer patients from undergoing ineffective irinotecan-based chemotherapy.

INTRODUCTION

Chemotherapy is still considered the backbone of anticancer therapy and has improved the life expectancy of countless patients (*1*, *2*). Unfortunately, a large fraction of patients do not benefit from this treatment but still experience substantial side effects (*3*–*6*). Although genomics has greatly facilitated patient selection for targeted therapies, this has been unsuccessful for chemotherapy, in part due to its often incompletely understood and diverse mechanisms of action (*7*–*9*). A handful of clinical parameters can help provide prognosis, but most of the proposed biomarkers are not currently used to predict chemotherapy treatment outcome in the clinic (*9*–*14*). Previous attempts to use patient material to determine treatment responsiveness have had limited success due to the long turnaround times, poor scalability, or low success rates of establishing patient cell lines or xenografts (*15*, *16*). Together, personalized cancer treatment for chemotherapy is currently lacking, and new predictive assays to help match patients to treatments are highly needed.

Patient-derived tumor organoids (PDOs) are cultures of tumor cells that can be derived from individual patients with a high success rate and expanded indefinitely, and which recapitulate morphological and genetic features of the original tumor (*17*–*19*). Recent post hoc studies suggest that PDOs may mirror clinical responses of individual patients to therapy (*20*, *21*). We therefore embarked on a multicenter, prospective, observational clinical study to determine the feasibility and potential value of PDOs as a predictive test for chemotherapy treatment regimens for colorectal cancer (CRC) patients. The Tumor Organoids: feasibility to predict sensitivity to treatment in cancer patients (TUMOROID) study is a multicenter study focused on regimens commonly used in CRC; patients received standard-of-care chemotherapy, including infusional 5-fluorouracil (5-FU) or capecitabine (oral prodrug of 5-FU), in combination with either oxaliplatin (referred to as FO) or irinotecan (FI), or irinotecan alone. Bevacizumab was allowed in all treatments, but patients who received additional cetuximab or panitumumab after the biopsy was taken were excluded. This criterion was chosen because the number of patients that received additional cetuximab or panitumumab was limited, and the selection based on wild-type *N/KRAS* would be a strong confounder. The primary objective was the development of an assay to accurately identify nonresponders to chemotherapy. Nonresponders were defined as patients with progressive disease (PD) after three cycles of chemotherapy according to the response evaluation criteria in solid tumors (RECIST) 1.1 (*22*).

RESULTS

Genetic and clinical characteristics of patients included in the TUMOROID study

We included 61 patients in the trial, from whom 67 biopsies were taken and cultured as previously described (*19*, *23*). Of the total 67 included biopsies, tissue retrieval was unsuccessful for four biopsies

[1]Department of Molecular Oncology and Immunology, Netherlands Cancer Institute, 1066 CX Amsterdam, Netherlands. [2]Oncode Institute, 3521 AL Utrecht, Netherlands. [3]Department of Biometrics, Netherlands Cancer Institute, 1066 CX Amsterdam, Netherlands. [4]Department of Molecular Carcinogenesis, Netherlands Cancer Institute, 1066 CX Amsterdam, Netherlands. [5]Department of Radiology, Netherlands Cancer Institute, 1066 CX Amsterdam, Netherlands. [6]Department of Pathology, Netherlands Cancer Institute, 1066 CX Amsterdam, Netherlands. [7]Department of Gastrointestinal Oncology, Netherlands Cancer Institute, 1066 CX Amsterdam, Netherlands. [8]Department of Internal Medicine/Oncology, Radboud University Medical Center Nijmegen, 6525 GA Nijmegen, Netherlands. [9]Department of Internal Medicine, Elisabeth-TweeSteden Hospital, 5042 AD Tilburg, Netherlands. [10]Faculty of Electrical Engineering, Mathematics and Computer Science, Delft University of Technology, 2628 CD Delft, Netherlands. [11]Division Biomedical Genetics, Centre for Molecular Medicine, University Medical Centre Utrecht, 3584 CX Utrecht, Netherlands. [12]Hartwig Medical Foundation, 1098 XH Amsterdam, Netherlands. [13]Hubrecht Institute, Royal Netherlands Academy of Arts and Sciences and University Medical Centre Utrecht, 3584 CT Utrecht, Netherlands. [14]Princess Máxima Center for Pediatric Oncology, 3584 CS Utrecht, Netherlands.
*These authors contributed equally to this work.
†These authors contributed equally to this work.
‡Present address: Department of Radiology and Nuclear Medicine, Amsterdam University Medical Center AMC, 1105 AZ Amsterdam, Netherlands.
§Corresponding author. Email: e.voest@nki.nl

Downloaded from http://stm.sciencemag.org/ by guest on July 22, 2021

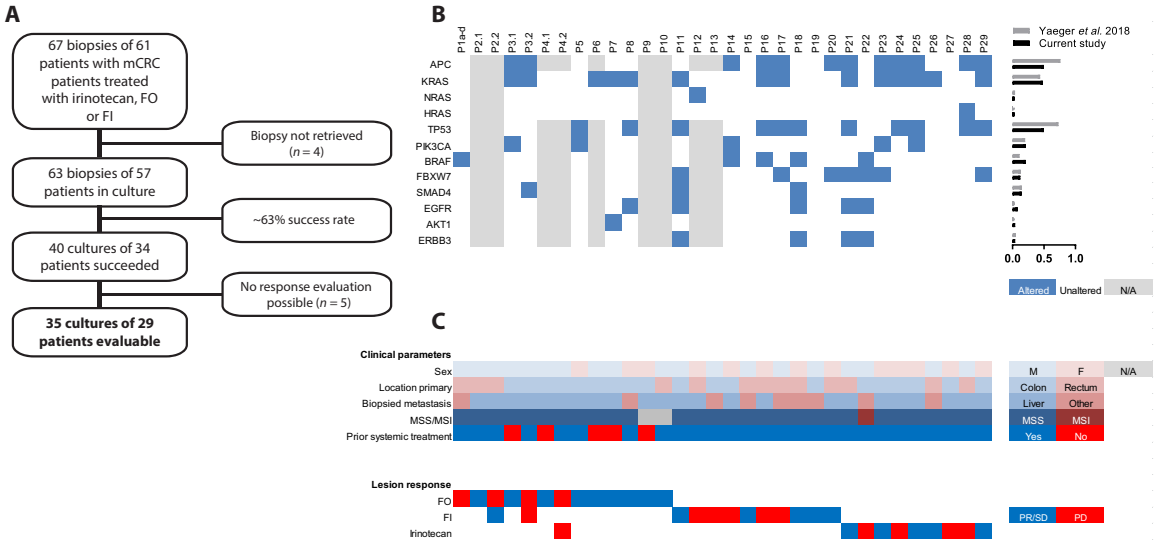

Fig. 1. Generation of PDOs from patients with metastatic CRC enrolled in the TUMOROID study. (**A**) Flow chart indicating the number of patients with metastatic CRC included, the number of evaluable patients, reasons for non-evaluability, and the success rate of establishing cultures from patients. (**B**) Overview of all patients, corresponding mutations in genes commonly mutated in CRC, and clinical parameters [sex, primary location, biopsied metastasis, microsatellite instability (MSI) status, and previous systemic treatment]. Gray boxes indicate that data were not available. On the right side are bar graphs representing the fraction of samples with a genetic aberration identified per gene, plotted and compared to those of Yaeger and colleagues (*24*). "Altered" was defined as a given variant being predicted pathogenic by COSMIC. (**C**) Clinical responses of patients, indicated in either blue (PR/SD) or red (PD), on the relevant treatment indicated on the left. The clinical and genetic data are described in more detail in tables S1 to S3.

(Fig. 1A). Culture of 23 of the remaining 63 biopsies failed due to no or too few tumor cells in the biopsy ($n = 14$), quality control problem ($n = 6$), or bacterial infection ($n = 3$). Overall, we obtained a ~63% PDO culture success rate (40 of 63 cultures) across the whole study, which is in line with previous reports (*18*–*20*), and found that clinical parameters did not influence culture success (fig. S1A). For five patients, the culture succeeded, but the clinical response was not evaluable, and therefore, the PDOs could not be used for in vitro patient comparison of drug response. Of the resulting 35 PDOs, 16 were used to evaluate the PDO drug sensitivity for first-line FO, and 22 were used for second-line FI or irinotecan (12 and 10 PDOs, respectively) (Fig. 1A). In most cases, the PDOs were established before the start of treatment. In rare cases, PDOs were established after progression on treatment (P27 and P28) or could also be used for testing response to multiple treatment outcomes because the patients were biopsied immediately after progression on first-line treatment with FO and right before the start of second-line treatment with irinotecan or FI (P2.2, P3.2, and P4.2). Patient and tumor characteristics, clinical background, pathological parameters, genetic aberrations, and treatment history are presented in Fig. 1B and more elaborately in tables S1 to S3. We found that the frequency of known genetic drivers of CRC was similar between the first (FO)– and second (FI/I)–line treatment cohorts (Fig. 1B) and similar to a recent clinical sequencing study of metastatic CRC, suggesting that our study describes a representative population of patients (*24*). Clinical response data for each patient are depicted in Fig. 1C.

PDOs predict response to irinotecan monotherapy

We first tested 10 PDOs from 10 patients treated with irinotecan (described in more detail in table S3). Five PDOs were derived from lesions that were classified as PD, and five were derived from lesions that were classified as stable disease (SD) (Fig. 2A; depicted in more detail in fig. S2A). This distribution of responses is in line with larger studies using irinotecan (*6*). All PDOs were exposed to the active metabolite of irinotecan, SN-38, for 6 days, and each screen was repeated by a second person to determine interobserver reproducibility (average Pearson's $R = 0.947$; range, 0.796 to 0.996; fig. S2B). We calculated the growth rate inhibition metrics (GR) of each condition 6 days after drug exposure and fitted dose-response curves (DRCs) (Fig. 2B) (*25*). We quantified responses to SN-38 by calculating the GR_{50} and the area under the DRC (AUC_{DRC}), both of which were significantly different between PDOs generated from PD versus SD lesions (Mann-Whitney test, $P = 0.0159$ and $P = 0.0079$, respectively; Fig. 2, C and D). To reduce the number of organoids and data points required for testing, we refined the drug assay by determining the concentration in the DRC at which the window of effect (or "variance") of chemosensitivity was the largest (fig. S3A). This strategy results in the elimination of drug concentrations for which the differential effect between PDOs was small. We found that 3.2 nM SN-38 yielded the largest window of effect, and PDOs from SD patients were more sensitive than PDOs from PD patients when exposed to this concentration (Mann-Whitney test, $P = 0.0159$; Fig. 2E and fig. S3A). The receiver operating characteristic (ROC) curve generated from this window had an AUC of 0.96 [confidence interval (CI), 0.8427 to 1.1077; Fig. 2F], comparable to those generated based on GR_{50} and AUC_{DRC} (summarized in Fig. 2G). We next aimed to develop a GR score–based classifier that accurately identifies nonresponders to irinotecan, without misclassifying responders, and test its predictive performance using leave-one-out cross-validation (LOOCV; fig. S3B). LOOCV resulted in correct classification of 80% of patients (empirical $P = 0.0061$; fig. S3B). These data demonstrate that PDOs have predictive value for irinotecan monotherapy, which can be captured by exposure to a single concentration of SN-38 and application of a cutoff of GR > 0.67. Such an assay only required ~5000 cells, which could be generated and screened within about 2 weeks.

Downloaded from http://stm.sciencemag.org/ by guest on July 22, 2021

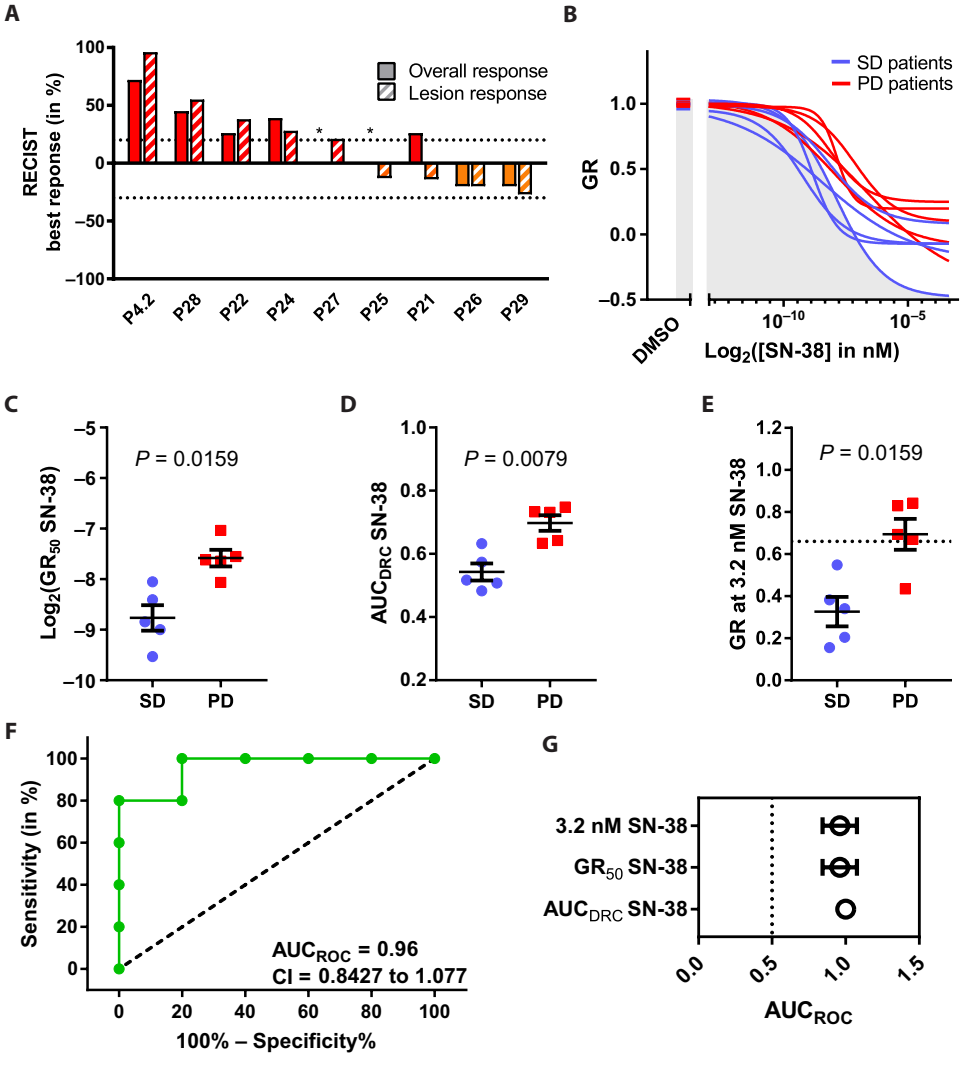

Fig. 2. PDO drug sensitivity predicts response to treatment with irinotecan. (**A**) Waterfall plot of each patient's overall response and best response of the biopsied lesion in the irinotecan-treated PDO cohort. Red indicates progressive disease (PD), and orange indicates stable disease (SD). *, new lesion(s). (**B**) Fitted dose-response curves (DRCs) of 10 PDOs exposed to SN-38 in vitro. Blue lines represent PDOs derived from SD patients, and red lines represent PDOs from PD patients. GR values represent in vitro sensitivity of PDOs to SN-38. The screen was plated in technical triplicate and performed twice, once each by independent researchers. Red indicates PD, and blue indicates SD. (**C**) $Log_2(GR_{50}$ SN-38) was interpolated from the fitted DRCs shown in (B). Groups were compared using a two-tailed Mann-Whitney test. Dots/squares represent individual PDOs, horizontal bars represent the mean, and error bars indicate SEM. (**D**) The area under the DRC (AUC_{DRC}) was calculated by integrating the DRC of each PDO in (B). Groups were compared using a two-tailed Mann-Whitney test. Dots/squares represent individual PDOs, horizontal bars represent the mean, and error bars indicate SEM. (**E**) The data point with the largest window of effect (captured by the variance) was calculated (3.2 nM SN-38; fig. S3A), and response was compared using a two-tailed Mann-Whitney test. (**F**) The data of (E) were plotted as an ROC curve. The dotted line represents an AUC_{ROC} of 0.5, which indicates no predictive value. CI, confidence interval. (**G**) Summary graph of the AUC_{ROC}s and 95% CIs on the basis of the in vitro parameters GR_{50} and AUC_{DRC}.

PDOs predict response to 5-FU–irinotecan combination therapy

Next, we attempted to construct a PDO-based classifier that would predict response to combination therapy. We also tested PDOs from 12 patients treated with FI (Fig. 3A; more details in fig. S4A). Again, the distribution of clinical responses was representative of distributions found in larger studies (*6*). Because FI is a combination chemotherapy of two drugs, we designed a drug matrix with a broad range of concentrations (fig. S4B). All 12 PDOs were screened in duplicate for response to FI (average Pearson's $R = 0.922$; range, 0.819 to 0.991; fig. S4C), and responses were quantified by summing the GR values across the drug matrix to create a "pan-matrix GR score" and then compared to the RECIST best response of the lesion (fig. S4D). We observed a pattern that closely mirrored the clinical responses: Five PDOs of patients with PD were resistant to FI in vitro, whereas seven PDOs derived from patients with partial response (PR)/SD were sensitive to FI (P14 was derived from a patient with PD but clustered with PDOs sensitive to FI; fig. S4D). Responses to the individual drugs 5-FU and SN-38 were not significantly different between PR/SD and PD lesions (fig. S4E). Most PDOs were either sensitive or resistant to both SN-38 and 5-FU, although there were two exceptions: P19 was resistant to 5-FU but sensitive to SN-38, and P20 showed the opposite. These data suggest that, in most cases, 5-FU and irinotecan collectively contribute to the effect of FI and the correlation found in vitro (fig. S4F).

Analogous to the method described for the irinotecan monotherapy cohort, we refined the drug assay by determining the concentrations in the drug matrix at which the variance of in vitro chemosensitivity was the largest (figs. S4B and S5A). This analysis identified two complementary rows and columns in the drug matrix with large windows of effect: 200 μM 5-FU as fixed concentration ("anchor") and a titration of SN-38, as well as 6.25 nM SN-38 as anchor and a titration of 5-FU (fig. S5A). For each PDO, we summed the 11 GR values within these two complementary DRCs to create a GR score and found these to differ between PR/SD and PD patients (Mann-Whitney test, $P = 0.0260$; Fig. 3B and fig. S5A). Furthermore, an ROC based on this score produced an AUC of 0.89 (Fig. 3C), suggesting that PDOs may have predictive value for FI combination chemotherapy. In addition, the 50% of PDOs that were most sensitive to FI in our assay had a significantly higher progression-free survival (PFS), indicating that in vitro sensitivity to FI is also associated with a longer response in the clinic (log-rank test, $P = 0.0278$; Fig. 3D). When compared to other in vitro endpoints, the combined DRCs performed as well as or better than 5-FU and SN-38 as single agents (summarized in Fig. 3E). Last, for clinical implementation, the two complementary DRCs of the FI assay only required ~10,000 cells,

Downloaded from http://stm.sciencemag.org/ by guest on July 22, 2021

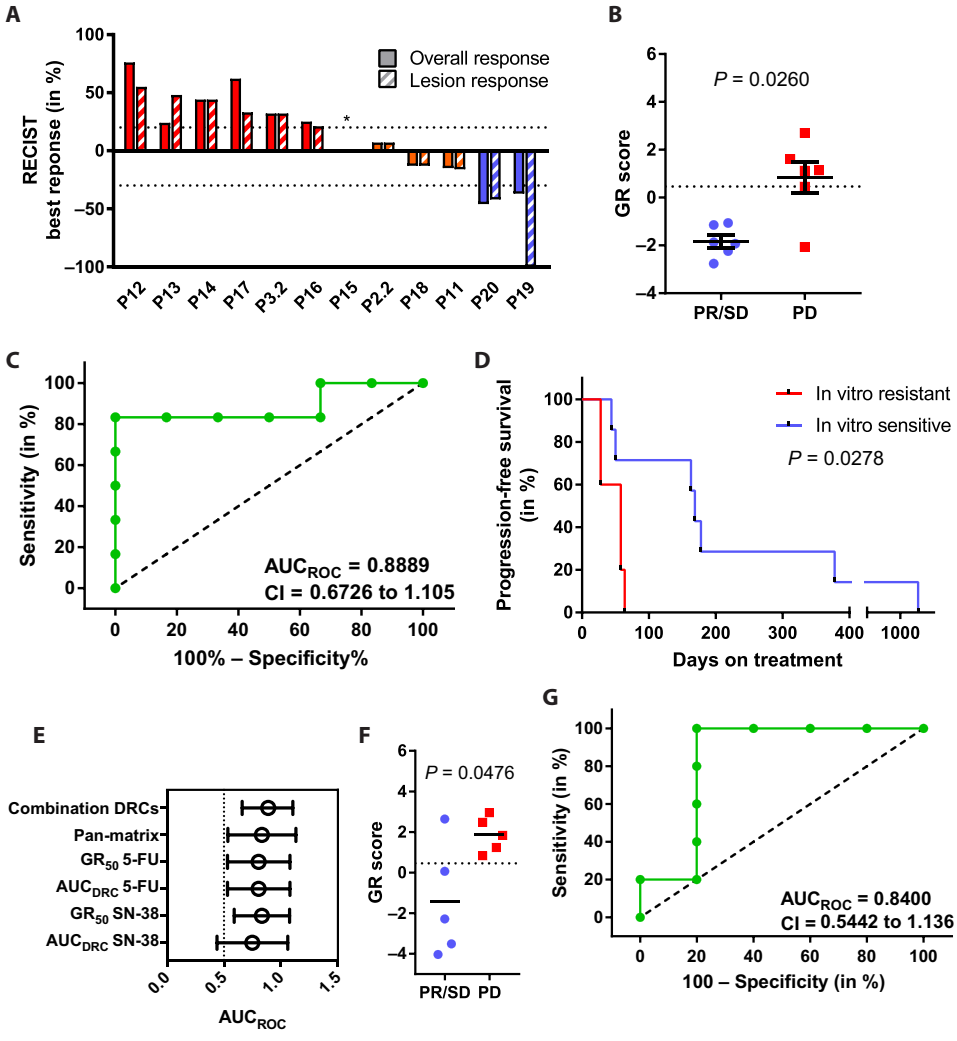

Fig. 3. PDO drug sensitivity predicts response to treatment with 5-FU/capecitabine and irinotecan. (**A**) Waterfall plot of each patient's overall response and best response of the biopsied lesion in the FI-treated PDO cohort. Red indicates PD, orange indicates SD, and blue indicates partial response (PR). *, new lesion(s). (**B**) GR scores of FI-treated PDOs derived from lesions with PR/SD and PD. Scores of PR/SD ($n = 6$) versus PD ($n = 6$) patients were compared using a two-tailed Mann-Whitney test. The screen was plated in technical triplicate and performed two times, once each by independent researchers. GR scores representing in vitro sensitivity of PDOs to FI were calculated by summing the 11 data points in the two complementary rows and columns in the drug matrix (fig. S5A). Dots/squares represent individual PDOs, horizontal bars represent the mean, and error bars indicate SEM. (**C**) ROC curve of the FI cohort illustrating the potential to predict response. AUC_{ROC} = area under the receiver operating characteristic curve. (**D**) Kaplan-Meier curve depicting the PFS of the 50% most sensitive versus 50% most resistant PDOs. Groups were compared using the Mantel-Cox log-rank test. (**E**) Summary of the AUC_{ROC} and 95% CI for lesion response, calculated based on the in vitro parameters GR_{50} and AUC_{DRC}. (**F**) GR scores of irinotecan-treated PDOs derived from lesions with PR/SD and PD. The test developed using the FI set [described in (B)] was applied to the 10 PDOs from the patients in the irinotecan monotherapy cohort: All PDOs were exposed to the 11 concentrations identified in (B), and GR scores representing in vitro sensitivity of PDOs to irinotecan were calculated analogous to the method described there. GR scores for PDO were compared to our threshold [GR > 0.46, represented by the dotted line in the figure, as identified previously in (B)] to determine whether PR/SD ($n = 5$) and PD ($n = 5$) patients were correctly classified by this method. Groups were compared using a two-tailed Fisher's exact test. (**G**) The data of (F) are plotted as an ROC curve.

which can be readily generated and screened within 21 days. This turnaround time is a marked improvement over the previously reported 2 to 6 months for other cell culture models and more similar to sequencing of gene panels such as the Memorial Sloan Kettering IMPACT panel (21 days) or the turnaround times reported in precision medicine studies (I-PREDICT median time to start treatment, ~29 days) (*15*, *26*, *27*).

To assess the performance of the FI classifier, we first repeated the LOOCV for the FI dataset and found that 83.3% of patients were correctly classified (empirical $P = 0.0017$; fig. S5B). We then tested the classifier for FI combination therapy on the cohort of patients described above, which received irinotecan monotherapy. All PDOs of the irinotecan cohort (Fig. 2A and fig. S2A) were exposed for 6 days to the complementary DRCs identified in the FI analysis above. When we applied the previously identified threshold of GR > 0.46, we correctly classified five of five resistant patients and four of five sensitive patients (90% correct; Fisher's exact test, $P = 0.0476$) (Fig. 3F). Furthermore, the ROC curve generated from this GR score had an AUC_{ROC} of 0.84 (Fig. 3G). Together, these results demonstrate the predictive nature of our test in a second patient cohort.

PDOs do not predict response to 5-FU–oxaliplatin combination therapy

We then performed similar experiments to test the predictive value of PDOs for FO chemotherapy using 16 PDOs derived from 10 patients (Fig. 4A and fig. S6A) (*22*). All samples were screened and analyzed as described above (inter-researcher reproducibility: average Pearson's $R = 0.971$; range, 0.935 to 0.996; fig. S6B). In contrast to the irinotecan-based patient cohorts, we did not find a notable difference in PDOs generated from PD versus PR/SD lesions in response to any of the tested parameters (Fig. 4B and fig. S6, C and D). Furthermore, no correlation with clinical response was found for the response to either the combination treatment or the individual drugs (summarized in fig. S6E). Consequently, the ROC curves showed no predictive value (Fig. 4, C and D).

To analyze intrapatient differences in drug responses before treatment (P1a-d) or over the course of treatment (P2 to P4), we calculated response to FO and individual drug responses of PDOs. Organoids were generated from multiple synchronous metastases of P1, as well as before and after treatment for P2 to P4. In line with a previous study, we found that responses to individual agents can differ substantially between lesions in a single patient (P1a-d; fig. S7, A and B) (*21*). However, all four lesions were comparably sensitive to the FO combination (fig. S7C), which contrasts with the heterogeneous responses to single agents (fig. S7, A and B, and summarized in fig. S7D). For three patients, we profiled drug

Downloaded from http://stm.sciencemag.org/ by guest on July 22, 2021

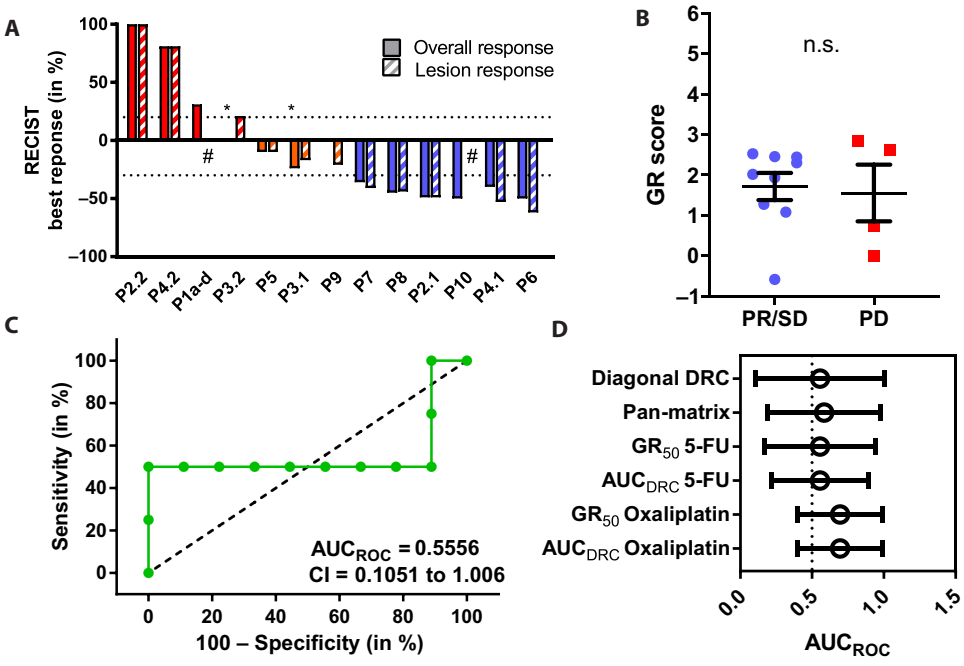

Fig. 4. PDO drug sensitivity does not predict response to treatment with 5-FU/capecitabine and oxaliplatin. (**A**) Waterfall plot of the best lesion and overall responses in the FO-treated PDO cohort. Red indicates PD, orange indicates SD, and blue indicates PR. *, new lesion(s); #, lesion could not be measured. (**B**) GR scores of FO-treated PDOs derived from lesions with PR/SD and PD. Scores of PR/SD ($n = 9$) versus PD ($n = 4$) patients were compared using a two-tailed Mann-Whitney test. The screen was plated in technical triplicate and performed two times, once each by independent researchers. GR scores representing in vitro sensitivity of PDOs to FO were calculated by summing the six data points of equimolar concentrations of 5-FU and oxaliplatin to generate a GR score. Dots/squares represent scores for individual PDOs (except for P1a-d, which are represented as the average of these four samples), horizontal bars represent the mean, and error bars represent the SEM. n.s., not significant. (**C**) ROC curve of the FO cohort illustrating the potential to predict response. (**D**) Summary graph of the AUC_{ROC}s and 95% CIs calculated on the basis of in vitro parameters GR_{50} and AUC_{DRC}.

responses before treatment and upon clinical progression to FO (fig. S7E). P2.1 showed a considerable response to single-agent 5-FU and oxaliplatin, and to the FO combination, which was partly diminished in P2.2 and mirrored the clinical response of this patients (fig. S7, E to H). This contrasts with P3 and P4, for whom only minor changes between pre- and posttreatment cultures were found in response to single-agent 5-FU and oxaliplatin and to the FO combination (fig. S7, F to H). Moreover, baseline sensitivity to FO varied greatly between P2, P3, and P4 (fig. S7F). These observations suggest that the current PDO culture/screening system does not recapitulate the responses of patients to FO in the clinic as it does for second-line irinotecan-based therapy.

We performed several calculations to control for underlying factors that might contribute to the discrepancy found between first-line (FO; $AUC_{ROC} = 0.5$) and second-line (FI/I; $AUC_{ROC} > 0.8$) therapy response in vitro. We calculated the interaction (odds ratio) of clinical parameters or the presence of mutations in common CRC driver genes with clinical response (fig. S8, A and B) or with individual PDO responses to chemotherapy (fig. S8, C and D). We did not find a significant association with response or resistance, either clinical or in vitro, for any of these parameters.

DISCUSSION

The discrepancy between the predictive value of PDOs for irinotecan-based treatment and FO suggests that the sensitivity and necessary conditions of the test might differ across types of chemotherapy and underscores our limited knowledge with regard to the mechanism of action of chemotherapy, especially in combinations. Plausible explanations include the absence of stroma and an immune system in PDO cultures, which can dictate treatment outcome in various ways (*8*). Culture methods that at least partially retain the patient tumor microenvironment in vitro might provide a platform to overcome this hurdle and offer valuable insight into the multilevel interaction of 5-FU and oxaliplatin (*23*, *28*). Another important factor in the clinical implementation of PDO-based tests is the culture success. Because culture is only successful for 63%, there is still a substantial fraction of patients for whom no PDO-informed decision can be made. Culture success might be further improved by obtaining multiple core biopsies, together with direct evaluation of the biopsies by a pathologist to identify samples with low cellularity, as suggested by Vlachogiannis *et al.* (*20*). Another technical limitation of functional tests is that they cannot be "rushed" as can be done for sequencing gene panels (*26*, *27*). These two points highlight the need to further increase the efficacy of PDO culture.

In summary, to date, there are no predictive tests for responsiveness to standard-of-care chemotherapy in CRC. Our data support the use of PDOs as a predictive tool to prospectively identify patients with metastatic CRC who would not benefit from irinotecan-based palliative chemotherapy. We have demonstrated that it is clinically feasible to use PDOs to deliver a prediction on the outcome of irinotecan-based chemotherapy. Although encouraged by the data, we are mindful of several limitations to our study. We have performed analyses (LOOCV, data randomization, testing of the FI assay in an irinotecan monotherapy cohort) to assess the strength of the data, but the number of patients on which our initial test was designed is limited, and the performances of the classifiers should be tested in independent cohorts of patients. However, we have now provided a foundation for confirmatory trials to validate and refine PDO-based tests and identify alternative treatments for patients unlikely to respond to irinotecan-based therapies (*20*, *21*). Our data suggest that it is clinically feasible to use PDOs to deliver a prediction for the outcome of irinotecan-based chemotherapy.

MATERIALS AND METHODS

Study design

The TUMOROID study is a Dutch multicenter observational cohort study (NL49002.031.14). The objective of the study was to evaluate the potential and feasibility of PDOs to distinguish patients with and without response to standard-of-care treatment, and the primary objective is a standardized PDO-based test with an AUC_{ROC}

Downloaded from http://stm.sciencemag.org/ by guest on July 22, 2021

of >0.7 and a high negative predictive value (the ability to exclude nonresponders without withholding treatment to responders). The study was approved by the ethical review board of the Netherlands Cancer Institute. The protocol complies with the Declaration of Helsinki, Dutch law, and Good Clinical Practice. All patients provided written informed consent before any study-related procedures. Patients with metastatic CRC were accrued at the Netherlands Cancer Institute, Meander Medical Centre Amersfoort, and Elisabeth-TweeSteden Hospital Tilburg. Eligibility criteria included an Eastern Cooperative Oncology Group performance status of ≤2, measurable disease, feasibility of tumor biopsy for histologic analysis, and age of 18 years or older. Patients underwent biopsies before start of treatment with clinically approved regimens of capecitabine/5-FU combined with oxaliplatin/irinotecan (described below). Patients were not randomized because the TUMOROID was an observational study. In select cases, posttreatment biopsies were obtained upon clinical progression. Patients underwent computed tomography scans at baseline and every 2 months to monitor response to treatment. Responses of the biopsied lesion were scored using RECIST 1.1 (*22*). All experiments were performed in parallel by two independent researchers. Researcher 2 was blinded to treatment outcome.

Treatment

Patients were treated according to clinically approved regimens of irinotecan monotherapy or capecitabine/5-FU in combination with oxaliplatin or irinotecan. Bevacizumab was allowed in all regimens, but patients receiving additional panitumumab or cetuximab were excluded. Irinotecan monotherapy (350 mg/m^2) was administered intravenously once every 3 weeks. Capecitabine plus oxaliplatin (CAPOX) was given in 3-week cycles; patients received capecitabine (1000 mg/m^2) orally twice a day on days 1 to 14 and oxaliplatin (130 mg/m^2) intravenously on day 1. 5-FU plus leucovorin plus oxaliplatin (FOLFOX) was given in 2-week cycles; patients received oxaliplatin (85 mg/m^2), leucovorin (400 mg/m^2), and 5-FU (400 mg/m^2 as a bolus, 600 mg/m^2 in 22 hours) intravenously on day 1. On day 2, the patients received leucovorin (200 mg/m^2) and 5-FU (400 mg/m^2 as a bolus, 600 mg/m^2 in 22 hours) intravenously. Capecitabine plus irinotecan (CAPIRI) was given in 3-week cycles, where patients received capecitabine (1000 mg/m^2) orally twice a day on days 1 to 14 and irinotecan (250 mg/m^2) intravenously on day 1. 5-FU plus leucovorin plus irinotecan (FOLFIRI) was given in cycles of 2 weeks; patients received irinotecan (180 mg/m^2), leucovorin (200 mg/m^2), and 5-FU (400 mg/m^2 as a bolus, 600 mg/m^2 in 22 hours) intravenously on day 1. On day 2, the patients received leucovorin (200 mg/m^2) and 5-FU (400 mg/m^2 as a bolus, 600 mg/m^2 in 22 hours) intravenously.

Patient material processing and organoid culture

One or two 18-gauge tumor biopsies were used for organoid culture and DNA sequencing. Biopsies were collected in Advanced Dulbecco's Modified Eagle's Medium with Nutrient Mixture Ham's F-12 (Ad-DF) (#12634, Invitrogen), supplemented with 1% penicillin-streptomycin (#15140-122, Invitrogen), 1% Hepes (#15630-056, Invitrogen), and 1% GlutaMAX (#35050, Invitrogen) (hereafter referred to as Ad-DF+++). Biopsies were stored for a maximum of 24 hours at 4°C before being dissociated with sharp needles. Cells were counted, washed with Ad-DF+++, and cultured as previously described in CRC growth medium (*17*, *23*). We could generally expand these biopsies to an average of ~2.0 × 10^5 cells at the first split (around day 10). PDO cultures were checked for mycoplasma contamination every month using the MycoAlert Mycoplasma Detection Kit (Lonza). As part of quality control, PDOs were authenticated using a TaqMan-based single-nucleotide polymorphism (SNP) array targeting 26 SNPs [Hartwig Medical Foundation (HMF)]. Identity scores of tumor DNA versus DNA obtained from healthy blood were computed as described elsewhere (*29*). PDOs with identity scores of <0.9 were discarded.

DNA sequencing

Part of the biopsied material of each patient was used for routine clinical sequencing of a panel of cancer genes (Illumina TruSeq; *ABL1*; *AKT1*; *ALK*; *APC*; *ATM*; *BRAF*; *CDH1*; *CDKN2A*; *CSF1R*; *CTNNB1*; *EGFR*; *ERBB2*; *ERBB4*; *FBXW7*; *FGFR1; FGFR2*; *FGFR3*; *FLT3*; *GNA11*; *GNAQ*; *GNAS*; *HNF1A*; *HRAS*; *ADH1*; *JAK2*; *JAK3*; *KDR*; *KIT*; *KRAS*; *MET*; *MLH1*; *MPL*; *NOTCH1*; *NPM1*; *NRAS*; *PDGFRA*; *PIK3CA*; *PTEN*; *PTPN11*; *RB1*; *RET*; *SMAD4*; *SMARCB1*; *SMO*; *SRC*; *STK11*; *TP53*; *VHL*) or whole-genome sequencing (WGS) by HMF. Both libraries were prepared according to the manufacturer's instructions (targeted sequencing: FC-130-1008; WGS: TruSeq Nano LT; FC-121-4001-3) and sequenced on the Illumina MiSeq (panel) or HiSeqX paired-end 2 × 150–base pair (WGS) platform. Analysis of the targeted panel was performed with Somatic Variant Caller v1.3 (Illumina). Analysis of the WGS data by the HMF was performed using their custom pipeline, which can be found online at BioRxiv/Github (*30*).

Drug screening

All drug screens were performed two times, once each by independent researchers. PDOs were mechanically and enzymatically dissociated into single cells by incubating in TrypLE (#12604-013, Gibco) for 5 to 10 min, filtered, and replated to allow for formation of organoids over the course of 4 days. After 4 days, PDOs were collected, incubated with dispase II (2 mg/ml; #D4693, Sigma) for 15 min to remove Geltrex, and counted using a hemocytometer and trypan blue. PDOs were resuspended in 1:2 Ad-DF+++:Geltrex at a concentration of 20 organoids/μl. Suspension (5 μl/well) was dispensed in clear-bottomed, white-walled 96-well plates (#3707, Corning) using an automated repeat pipet and overlaid with 200 μl of CRC growth medium. We generated six-step, fourfold drug matrices of 5-FU + oxaliplatin or 5-FU + SN-38 and 10-step, twofold single-drug DRCs in technical triplicate, covering physiological concentrations of 5-FU (5-FU C_{max} in patients = 1.7 to 2.4 μM; 5-FU range in vitro = 0.319 to 200 μM), SN-38 (C_{max} in patients ≈ 26 nM; SN-38 range in vitro = 0.195 to 100 nM), and oxaliplatin (oxaliplatin C_{max} in patients = 3.8 to 10.1 μM; oxaliplatin range in vitro = 0.319 to 200 μM) in patients using a Tecan D300e digital dispenser (*31*–*33*). Readouts were obtained at day 0 ("baseline") and at day 6 in the positive control (10 μM phenylarsine oxide), negative control, and the drug-treated wells. Experiments that had poor or low cell growth (defined as less than twofold growth over 6 days) were excluded. Quantification of cell viability was done by replacing the CRC growth medium with 50 μl of CellTiter-Glo 3D (#G9681, Promega) mixed with 50 μl of Ad-DF+++ according to the manufacturer's instructions on an Infinite 200 Pro plate reader (Tecan Life Sciences).

DRC fitting and correlation analysis

For P1a-d, the results reported are the average of the four samples. In cases where lesion response could not be accurately measured (P1 and P10), overall response was used. GRs were calculated on the

Downloaded from http://stm.sciencemag.org/ by guest on July 22, 2021

basis of median luminescence values of day 0, untreated day 6, and drug-treated wells at day 6, using the method described in more detail elsewhere (*24*). For the FI cohort, the GR value of each data point in the whole drug combination matrix or two DRCs (200 μM 5-FU anchor plus a titration of SN-38 combined with 6.25 nM SN-38 anchor and a titration of 5-FU) was summed to create a GR score for each PDO line. *Z*-scores used in the Kaplan-Meier curve were calculated as $(\mu - X)/\sigma$ (μ, mean; *X*, score; σ, SD). Scores for response to combined FO in vitro were calculated on the basis of the 1:1 ratio (the "diagonal" in the combination matrix) of FO, again summing the GR value of each point to create an overall score. Curve fitting and estimation of GR_{50}s was done using the GRmetrics package v.1.8.0 in R (*34*). AUC_{DRC}s were inferred by integrating fitted curves. To analyze the reproducibility between drug screen 1 and drug screen 2, we calculated Pearson's *R* and corresponding *P* value using either the GR value of the 11 data points in two complementary rows and columns identified as having the largest variance within our samples (FI cohort) or the GR value of the 36 data points in the full combination matrix (FO cohort) or all 10 data points in the DRCs (irinotecan monotherapy cohort). Correlation analyses, with associated *P* values, were performed using the COR function in R.

LOOCV and data randomization

To identify data points that had the largest variance within our samples in the irinotecan set, we calculated the variance for each of the 10 data points in the DRCs, across all 10 PDOs, in a leave-one-out setting. To set the threshold for the irinotecan classifier, we selected the GR score within our set of 10 samples that correctly classified all sensitive patients while correctly classifying the maximum number of resistant patients (GR > 0.76 classified as resistant; Fig. 2E).

To test the predictive performance of this threshold, we applied LOOCV and data randomization. Here, we used nine samples as a training set to identify the data point with the highest variance, as described above. Next, we randomly reassigned our 10 GR scores among five sensitive and five resistant "patients." Using the GR scores of the nine training samples, we set a threshold and used this cutoff to classify the 10th (validation) sample as either sensitive or resistant (fig. S3, A and B). In this manner, tested samples were never used to determine the threshold. As with our empirically determined threshold, we set the threshold by selecting the highest GR score that correctly classified all sensitive patients within the test set of nine PDOs while correctly classifying the maximum number of resistant patients within the test set of nine PDOs. Within each loop, the data randomization step was performed 120,000 times. This entire procedure was repeated 10 times in total, each time leaving out a different PDO. The *P* value for our empirically determined threshold was calculated by dividing the number of cases where a randomly generated classifier threshold performed as well as, or better than, our empirically determined classifier threshold by the number of iterations executed ($P = R/I$; *P* is the *P* value; *R* is the number of times random data outperform our classifier; *I* is the number of iterations executed).

The analysis of the FI set was performed in a similar manner: We identified two complementary DRCs that had the largest variance within our samples in the FI set by calculating the variance for each of the 36 data points in the full drug matrix, across all 12 PDOs, in a leave-one-out setting. To set the threshold for the FI classifier, we selected the GR score within our set of 12 samples that correctly classified all sensitive patients while correctly classifying the maximum number of resistant patients (GR > 0.46 classified as resistant; Fig. 3B).

To test the predictive performance of this threshold, we applied LOOCV and data randomization. Here, we used 11 samples as a training set to identify the two complementary DRCs with the highest variance, as described above. Then, for each of our 12 PDOs, the GR score was determined by summing the GR value of the 11 data points within these two complementary DRCs. Next, we randomly reassigned our 12 GR scores among six sensitive and six resistant patients. Using the GR scores of the 11 training samples, we set a threshold and used this cutoff to classify the 12th (validation) sample as either sensitive or resistant (fig. S5, A and B). In this manner, tested samples were never used to determine the threshold. As with our empirically determined threshold, we set the threshold by selecting the highest GR score that correctly classified all sensitive patients within the test set of 11 PDOs while correctly classifying the maximum number of resistant patients within the test set of 11 PDOs. Within each loop, the data randomization step was performed 120,000 times. This entire procedure was repeated 12 times in total, each time leaving out a different PDO. The *P* value for our empirically determined threshold was calculated by dividing the number of cases where a randomly generated classifier threshold performed as well as, or better than, our empirically determined classifier threshold by the number of iterations executed.

Statistical analysis

Groups were compared using a Mann-Whitney test in case of continuous variables and Fisher's exact test in case of categorical values. The Mann-Whitney test was applied because data were not normally distributed, and Fisher's exact test was applied because of the relatively small sample size. Difference in PFS was calculated using the log-rank test. Concordance between replicates was calculated using Pearson's *R*. All statistical tests were performed two-tailed in GraphPad Prism V7.03, with the exception of the correlation analysis, which was done in *R*. *P* values were corrected for multiple testing using Bonferroni correction when required, as mentioned in the figure legends. *P* values of <0.05 were considered significant.

SUPPLEMENTARY MATERIALS

stm.sciencemag.org/cgi/content/full/11/513/eaay2574/DC1
Fig. S1. Overview of clinical and genetic parameters in PDO cohorts.
Fig. S2. Overview of the irinotecan PDO-patient cohort.
Fig. S3. Development and cross-validation of an irinotecan classifier.
Fig. S4. Overview of the 5-FU–irinotecan PDO-patient cohort.
Fig. S5. Development and cross-validation of a 5-FU–irinotecan classifier.
Fig. S6. Overview of the 5-FU–oxaliplatin PDO-patient cohort.
Fig. S7. 5-FU–oxaliplatin drug responses of synchronous and paired metastases.
Fig. S8. The effects of clinical and genetic parameters on patients and PDO responses.
Table S1. Characteristics and clinical history of all patients included in the TUMOROID study.
Table S2. Genetic and pathological characteristics of patients in the TUMOROID study.
Table S3. Overview of the three cohorts and previous treatments and procedures.
View/request a protocol for this paper from *Bio-protocol*.

REFERENCES AND NOTES

1. K. D. Miller, R. L. Siegel, C. C. Lin, A. B. Mariotto, J. L. Kramer, J. H. Rowland, K. D. Stein, R. Alteri, A. Jemal, Cancer treatment and survivorship statistics, 2016. *CA Cancer J. Clin.* **66**, 271–289 (2016).
2. A. Grothey, D. Sargent, R. M. Goldberg, H.-J. Schmoll, Survival of patients with advanced colorectal cancer improves with the availability of fluorouracil-leucovorin, irinotecan, and oxaliplatin in the course of treatment. *J. Clin. Oncol.* **22**, 1209–1214 (2004).
3. H. G. Prigerson, Y. Bao, M. A. Shah, M. E. Paulk, T. W. LeBlanc, B. J. Schneider, M. M. Garrido, M. C. Reid, D. A. Berlin, K. B. Adelson, A. I. Neugut, P. K. Maciejewski, Chemotherapy use, performance status, and quality of life at the end of life. *JAMA Oncol.* **1**, 778–784 (2015).

Downloaded from http://stm.sciencemag.org/ by guest on July 22, 2021

4. J. Cassidy, J. Tabernero, C. Twelves, R. Brunet, C. Butts, T. Conroy, F. Debraud, A. Figer, J. Grossmann, N. Sawada, P. Schöffski, A. Sobrero, E. van Cutsem, E. Díaz-Rubio, XELOX (capecitabine plus oxaliplatin): Active first-line therapy for patients with metastatic colorectal cancer. *J. Clin. Oncol.* **22**, 2084–2091 (2004).
5. C. Tournigand, T. André, E. Achille, G. Lledo, M. Flesh, D. Mery-Mignard, E. Quinaux, C. Couteau, M. Buyse, G. Ganem, B. Landi, P. Colin, C. Louvet, A. de Gramont, FOLFIRI followed by FOLFOX6 or the reverse sequence in advanced colorectal cancer: A randomized GERCOR study. *J. Clin. Oncol.* **22**, 229–237 (2004).
6. M. T. Seymour, T. S. Maughan, J. A. Ledermann, C. Topham, R. James, S. J. Gwyther, D. B. Smith, S. Shepherd, A. Maraveyas, D. R. Ferry, A. M. Meade, L. Thompson, G. O. Griffiths, M. K. B. Parmar, R. J. Stephens; FOCUS Trial Investigators; National Cancer Research Institute Colorectal Clinical Studies Group, Different strategies of sequential and combination chemotherapy for patients with poor prognosis advanced colorectal cancer (MRC FOCUS): A randomised controlled trial. *Lancet* **370**, 143–152 (2007).
7. C. Holohan, S. Van Schaeybroeck, D. B. Longley, P. G. Johnston, Cancer drug resistance: An evolving paradigm. *Nat. Rev. Cancer* **13**, 714–726 (2013).
8. L. Zitvogel, L. Apetoh, F. Ghiringhelli, G. Kroemer, Immunological aspects of cancer chemotherapy. *Nat. Rev. Immunol.* **8**, 59–73 (2008).
9. C. J. A. Punt, M. Koopman, L. Vermeulen, From tumour heterogeneity to advances in precision treatment of colorectal cancer. *Nat. Rev. Clin. Oncol.* **14**, 235–246 (2017).
10. M. P. A. Ebert, M. Tänzer, B. Balluff, E. Burgermeister, A. K. Kretzschmar, D. J. Hughes, R. Tetzner, C. Lofton-Day, R. Rosenberg, A. C. Reinacher-Schick, K. Schulmann, A. Tannapfel, R. Hofheinz, C. Röcken, G. Keller, R. Langer, K. Specht, R. Porschen, J. Stöhlmacher-Williams, T. Schuster, P. Ströbel, R. M. Schmid, *TFAP2E–DKK4* and chemoresistance in colorectal cancer. *N. Engl. J. Med.* **366**, 44–53 (2012).
11. C. G. Leichman, H. J. Lenz, L. Leichman, K. Danenberg, J. Baranda, S. Groshen, W. Boswell, R. Metzger, M. Tan, P. V. Danenberg, Quantitation of intratumoral thymidylate synthase expression predicts for disseminated colorectal cancer response and resistance to protracted-infusion fluorouracil and weekly leucovorin. *J. Clin. Oncol.* **15**, 3223–3229 (1997).
12. C. Aschele, D. Debernardis, S. Casazza, G. Antonelli, G. Tunesi, C. Baldo, R. Lionetto, F. Maley, A. Sobrero, Immunohistochemical quantitation of thymidylate synthase expression in colorectal cancer metastases predicts for clinical outcome to fluorouracil-based chemotherapy. *J. Clin. Oncol.* **17**, –1760, 1770 (1999).
13. M. J. Garnett, E. J. Edelman, S. J. Heidorn, C. D. Greenman, A. Dastur, K. W. Lau, P. Greninger, I. R. Thompson, X. Luo, J. Soares, Q. Liu, F. Iorio, D. Surdez, L. Chen, R. J. Milano, G. R. Bignell, A. T. Tam, H. Davies, J. A. Stevenson, S. Barthorpe, S. R. Lutz, F. Kogera, K. Lawrence, A. McLaren-Douglas, X. Mitropoulos, T. Mironenko, H. Thi, L. Richardson, W. Zhou, F. Jewitt, T. Zhang, P. O'Brien, J. L. Boisvert, S. Price, W. Hur, W. Yang, X. Deng, A. Butler, H. G. Choi, J. W. Chang, J. Baselga, I. Stamenkovic, J. A. Engelman, S. V. Sharma, O. Delattre, J. Saez-Rodriguez, N. S. Gray, J. Settleman, P. A. Futreal, D. A. Haber, M. R. Stratton, S. Ramaswamy, U. McDermott, C. H. Benes, Systematic identification of genomic markers of drug sensitivity in cancer cells. *Nature* **483**, 570–575 (2012).
14. J. Barretina, G. Caponigro, N. Stransky, K. Venkatesan, A. A. Margolin, S. Kim, C. J. Wilson, J. Lehár, G. V. Kryukov, D. Sonkin, A. Reddy, M. Liu, L. Murray, M. F. Berger, J. E. Monahan, P. Morais, J. Meltzer, A. Korejwa, J. Jané-Valbuena, F. A. Mapa, J. Thibault, E. Bric-Furlong, P. Raman, A. Shipway, I. H. Engels, J. Cheng, G. K. Yu, J. Yu, P. Aspesi, M. de Silva, K. Jagtap, M. D. Jones, L. Wang, C. Hatton, E. Palescandolo, S. Gupta, S. Mahan, C. Sougnez, R. C. Onofrio, T. Liefeld, L. MacConaill, W. Winckler, M. Reich, N. Li, J. P. Mesirov, S. B. Gabriel, G. Getz, K. Ardlie, V. Chan, V. E. Myer, B. L. Weber, J. Porter, M. Warmuth, P. Finan, J. L. Harris, M. Meyerson, T. R. Golub, M. P. Morrissey, W. R. Sellers, R. Schlegel, L. A. Garraway, The Cancer Cell Line Encyclopedia enables predictive modelling of anticancer drug sensitivity. *Nature* **483**, 603–607 (2012).
15. A. S. Crystal, A. T. Shaw, L. V. Sequist, L. Friboulet, M. J. Niederst, E. L. Lockerman, R. L. Frias, J. F. Gainor, A. Amzallag, P. Greninger, D. Lee, A. Kalsy, M. Gomez-Caraballo, L. Elamine, E. Howe, W. Hur, E. Lifshits, H. E. Robinson, R. Katayama, A. C. Faber, M. M. Awad, S. Ramaswamy, M. Mino-Kenudson, A. J. Iafrate, C. H. Benes, J. A. Engelman, Patient-derived models of acquired resistance can identify effective drug combinations for cancer. *Science* **346**, 1480–1486 (2014).
16. A. A. Friedman, A. Letai, D. E. Fisher, K. T. Flaherty, Precision medicine for cancer with next-generation functional diagnostics. *Nat. Rev. Cancer* **15**, 747–756 (2015).
17. T. Sato, D. E. Stange, M. Ferrante, R. G. J. Vries, J. H. van Es, S. van den Brink, W. J. van Houdt, A. Pronk, J. van Gorp, P. D. Siersema, H. Clevers, Long-term expansion of epithelial organoids from human colon, adenoma, adenocarcinoma, and Barrett's epithelium. *Gastroenterology* **141**, 1762–1772 (2011).
18. J. Drost, H. Clevers, Organoids in cancer research. *Nat. Rev. Cancer* **18**, 407–418 (2018).
19. F. Weeber, M. van de Wetering, M. Hoogstraat, K. K. Dijkstra, O. Krijgsman, T. Kuilman, C. G. M. Gadellaa-van Hooijdonk, D. L. van der Velden, D. S. Peeper, E. P. J. G. Cuppen, R. G. Vries, H. Clevers, E. E. Voest, Preserved genetic diversity in organoids cultured from biopsies of human colorectal cancer metastases. *Proc. Natl. Acad. Sci. U.S.A.* **112**, 13308–13311 (2015).
20. G. Vlachogiannis, S. Hedayat, A. Vatsiou, Y. Jamin, J. Fernández-Mateos, K. Khan, A. Lampis, K. Eason, I. Huntingford, R. Burke, M. Rata, D. M. Koh, N. Tunariu, D. Collins, S. Hulkki-Wilson, C. Ragulan, I. Spiteri, S. Y. Moorcraft, I. Chau, S. Rao, D. Watkins, N. Fotiadis, M. Bali, M. Darvish-Damavandi, H. Lote, Z. Eltahir, E. C. Smyth, R. Begum, P. A. Clarke, J. C. Hahne, M. Dowsett, J. de Bono, P. Workman, A. Sadanandam, M. Fassan, O. J. Sansom, S. Eccles, N. Starling, C. Braconi, A. Sottoriva, S. P. Robinson, D. Cunningham, N. Valeri, Patient-derived organoids model treatment response of metastatic gastrointestinal cancers. *Science* **359**, 920–926 (2018).
21. H. Tiriac, P. Belleau, D. D. Engle, D. Plenker, A. Deschênes, T. D. D. Somerville, F. E. M. Froeling, R. A. Burkhart, R. E. Denroche, G.-H. Jang, K. Miyabayashi, C. Megan Young, H. Patel, M. Ma, J. F. LaComb, R. L. D. Palmaira, A. A. Javed, J. A. Huynh, M. Johnson, K. Arora, N. Robine, M. Shah, R. Sanghvi, A. B. Goetz, C. Y. Lowder, L. Martello, E. Driehuis, N. Lecomte, G. Askan, C. A. Iacobuzio-Donahue, H. Clevers, L. D. Wood, R. H. Hruban, E. D. Thompson, A. J. Aguirre, B. M. Wolpin, A. Sasson, J. Kim, M. Wu, J. C. Bucobo, P. J. Allen, D. V. Sejpal, W. Nealon, J. D. Sullivan, J. M. Winter, P. A. Gimotty, J. L. Grem, D. J. DiMaio, J. M. Buscaglia, P. M. Grandgenett, J. R. Brody, M. A. Hollingsworth, G. M. O'Kane, F. Notta, E. J. Kim, J. M. Crawford, C. E. Devoe, A. Ocean, C. L. Wolfgang, K. H. Yu, E. Li, C. R. Vakoc, B. Hubert, S. E. Fischer, J. M. Wilson, R. A. Moffitt, J. J. Knox, A. Krasnitz, S. Gallinger, D. A. Tuveson, Organoid profiling identifies common responders to chemotherapy in pancreatic cancer. *Cancer Discov.* **8**, 1112–1129 (2018).
22. E. A. Eisenhauer, P. Therasse, J. Bogaerts, L. H. Schwartz, D. Sargent, R. Ford, J. Dancey, S. Arbuck, S. Gwyther, M. Mooney, L. Rubinstein, L. Shankar, L. Dodd, R. Kaplan, D. Lacombe, J. Verweij, New response evaluation criteria in solid tumours: Revised RECIST guideline (version 1.1). *Eur. J. Cancer* **45**, 228–247 (2009).
23. K. K. Dijkstra, C. M. Cattaneo, F. Weeber, M. Chalabi, J. van de Haar, L. F. Fanchi, M. Slagter, D. L. van der Velden, S. Kaing, S. Kelderman, N. van Rooij, M. E. van Leerdam, A. Depla, E. F. Smit, K. J. Hartemink, R. de Groot, M. C. Wolkers, N. Sachs, P. Snaebjornsson, K. Monkhorst, J. Haanen, H. Clevers, T. N. Schumacher, E. E. Voest, Generation of tumor-reactive T cells by co-culture of peripheral blood lymphocytes and tumor organoids. *Cell* **174**, 1586–1598.e12 (2018).
24. R. Yaeger, W. K. Chatila, M. D. Lipsyc, J. F. Hechtman, A. Cercek, F. Sanchez-Vega, G. Jayakumaran, S. Middha, A. Zehir, M. T. A. Donoghue, D. You, A. Viale, N. Kemeny, N. H. Segal, Z. K. Stadler, A. M. Varghese, R. Kundra, J. Gao, A. Syed, D. M. Hyman, E. Vakiani, N. Rosen, B. S. Taylor, M. Ladanyi, M. F. Berger, D. B. Solit, J. Shia, L. Saltz, N. Schultz, Clinical sequencing defines the genomic landscape of metastatic colorectal cancer. *Cancer Cell* **33**, 125–136.e3 (2018).
25. M. Hafner, M. Niepel, M. Chung, P. K. Sorger, Growth rate inhibition metrics correct for confounders in measuring sensitivity to cancer drugs. *Nat. Methods* **13**, 521–527 (2016).
26. A. Zehir, R. Benayed, R. H. Shah, A. Syed, S. Middha, H. R. Kim, P. Srinivasan, J. Gao, D. Chakravarty, S. M. Devlin, M. D. Hellmann, D. A. Barron, A. M. Schram, M. Hameed, S. Dogan, D. S. Ross, J. F. Hechtman, D. F. DeLair, J. J. Yao, D. L. Mandelker, D. T. Cheng, R. Chandramohan, A. S. Mohanty, R. N. Ptashkin, G. Jayakumaran, M. Prasad, M. H. Syed, A. B. Rema, Z. Y. Liu, K. Nafa, L. Borsu, J. Sadowska, J. Casanova, R. Bacares, I. J. Kiecka, A. Razumova, J. B. Son, L. Stewart, T. Baldi, K. A. Mullaney, H. al-Ahmadie, E. Vakiani, A. A. Abeshouse, A. V. Penson, P. Jonsson, N. Camacho, M. T. Chang, H. H. Won, B. E. Gross, R. Kundra, Z. J. Heins, H. W. Chen, S. Phillips, H. Zhang, J. Wang, A. Ochoa, J. Wills, M. Eubank, S. B. Thomas, S. M. Gardos, D. N. Reales, J. Galle, R. Durany, R. Cambria, W. Abida, A. Cercek, D. R. Feldman, M. M. Gounder, A. A. Hakimi, J. J. Harding, G. Iyer, Y. Y. Janjigian, E. J. Jordan, C. M. Kelly, M. A. Lowery, L. G. T. Morris, A. M. Omuro, N. Raj, P. Razavi, A. N. Shoushtari, N. Shukla, T. E. Soumerai, A. M. Varghese, R. Yaeger, J. Coleman, B. Bochner, G. J. Riely, L. B. Saltz, H. I. Scher, P. J. Sabbatini, M. E. Robson, D. S. Klimstra, B. S. Taylor, J. Baselga, N. Schultz, D. M. Hyman, M. E. Arcila, D. B. Solit, M. Ladanyi, M. F. Berger, Mutational landscape of metastatic cancer revealed from prospective clinical sequencing of 10,000 patients. *Nat. Med.* **23**, 703–713 (2017).
27. J. K. Sicklick, S. Kato, R. Okamura, M. Schwaederle, M. E. Hahn, C. B. Williams, P. de, A. Krie, D. E. Piccioni, V. A. Miller, J. S. Ross, A. Benson, J. Webster, P. J. Stephens, J. J. Lee, P. T. Fanta, S. M. Lippman, B. Leyland-Jones, R. Kurzrock, Molecular profiling of cancer patients enables personalized combination therapy: The I-PREDICT study. *Nat. Med.* **25**, 744–750 (2019).
28. J. T. Neal, X. Li, J. Zhu, V. Giangarra, C. L. Grzeskowiak, J. Ju, I. H. Liu, S.-H. Chiou, A. A. Salahudeen, A. R. Smith, B. C. Deutsch, L. Liao, A. J. Zemek, F. Zhao, K. Karlsson, L. M. Schultz, T. J. Metzner, L. D. Nadauld, Y. Y. Tseng, S. Alkhairy, C. Oh, P. Keskula, D. Mendoza-Villanueva, F. M. de la Vega, P. L. Kunz, J. C. Liao, J. T. Leppert, J. B. Sunwoo, C. Sabatti, J. S. Boehm, W. C. Hahn, G. X. Y. Zheng, M. M. Davis, C. J. Kuo, Organoid modeling of the tumor immune microenvironment. *Cell* **175**, 1972–1988.e16 (2018).
29. M. M. Y. Liang-Chu, M. Yu, P. M. Haverty, J. Koeman, J. Ziegle, M. Lee, R. Bourgon, R. M. Neve, Human biosample authentication using the high-throughput, cost-effective SNPtrace™ system. *PLOS ONE* **10**, e0116218 (2015).
30. P. Priestley, J. Baber, M. P. Lolkema, N. Steeghs, E. de Bruijn, K. Duyvesteyn, S. Haidari, A. van Hoeck, W. Onstenk, P. Roepman, C. Shale, M. Voda, H. J. Bloemendal,

Downloaded from http://stm.sciencemag.org/ by guest on July 22, 2021

V. C. G. Tjan-Heijnen, C. M. L. van Herpen, M. Labots, P. O. Witteveen, E. F. Smit, S. Sleijfer, E. E. Voest, E. Cuppen, Pan-cancer whole genome analyses of metastatic solid tumors. bioRxiv 415133 [**Preprint**]. 20 September 2018.
31. B. Reigner, K. Blesch, E. Weidekamm, Clinical pharmacokinetics of capecitabine. *Clin. Pharmacokinet.* **40**, 85–104 (2001).
32. M. A. Graham, G. F. Lockwood, D. Greenslade, S. Brienza, M. Bayssas, E. Gamelin, Clinical pharmacokinetics of oxaliplatin: A critical review. *Clin. Cancer Res.* **6**, 1205–1218 (2000).
33. G. G. Chabot, Clinical pharmacokinetics of irinotecan. *Clin. Pharmacokinet.* **33**, 245–259 (1997).

Acknowledgments: We would like to acknowledge C. Cattaneo, C. Stangl, R. Bernards, D. Peeper, D. Vredevoogd, P. Borst, H. Snippert, S. Boj, M. van de Wetering, and R. Overmeer for useful discussions and advice. We would also like to thank M. Schrier for monitoring the study and, in particular, J.-N. Ridderbos and D. Hunneman for handling biopsy specimens, E. Platte for the study blood withdrawals, the scientific administration of the NKI-AvL and L. Wever, G. de Jong, and M. Chung for registration of study patients and data management, as well as P. Hagen and D. Baars for construction of the electronic case-report files (eCRF) of the IKNL for data management of patients who were included in other hospitals. We would like to acknowledge S. van Lieshout and E. de Bruijn for performing authentication of PDOs and S. van der Kolk, J. Westra, and S. Visser for help with patient inclusion. R-spondin1–producing cells were a gift from C. Kuo (Stanford University). We also thank K. Jozwiack and K. Sikorska for input on statistical analysis and B. Morris and the Netherlands Cancer Institute (NKI) Robotics and Screening Facility for advice on experimental design and all other research facilities at the NKI for their contribution and help. Furthermore, we would like to thank all participating centers, medical oncologists, and patients for contributing to the study. **Funding:** This study was supported by grants from the Koningin Wilhelmina Fonds (KWF; E.E.V.; NKI2015-7732 and HUBR2014-7006) and the Nederlands Wetenschappelijk Orgaan (NWO) gravitation program (E.E.V.; 2012–2022; on behalf of www.CancerGenomiCs.nl.
Author contributions: S.N.O. and C.M.M. designed and performed experiments, analyzed the data, and wrote the paper with input from all authors. S.N.O. and E.E.V. revised the manuscript. F.W. coordinated the clinical trial. K.K.D. contributed to the design and conceptual basis of the study. S.K. provided technical assistance in establishing, culturing, and expanding PDOs. E.v.W. contributed to the statistical design. L.H. and L.S. provided assistance in coordinating the clinical trial. D.J.V. assisted in analysis of the drug response data. J.v.d.H. contributed to the analysis. W.P. and P.S. provided radiological/pathological expertise. D.v.d.V. provided assistance in coordinating the clinical trial. M.K. performed experiments. M.C., H.B., M.v.L., H.J.B., and L.V.B. included patients. L.W. provided bioinformatics expertise. E.C. coordinated WGS. H.C. contributed to the design and conceptual basis of the study. E.E.V. contributed to the (experimental) design and conceptual basis of the study, and supervised the overall execution of the study. **Competing interests:** E.E.V. is the medical director of the Netherlands Cancer Institute. E.E.V. and S.N.O. are inventors on patent application EP18207636.4 submitted by Stichting Het Nederlands Kanker Instituut—Antoni van Leeuwenhoek Ziekenhuis that covers a method of predicting responsiveness of a gastrointestinal cancer patient to a chemotherapy treatment. H.C. is an inventor on several patents regarding organoid culture and a cofounder and scientific advisory board member of Surrozen. H.C. is a scientific advisory board (SAB) member of the biotech firms Kallyope (New York), Merus (Utrecht), and Decibel (Boston). H.C. is a non-executive board member of Roche (Basel) and SAB member of the Roche subsidiary Genentech (San Francisco) since 2019. H.C. is a scientific advisor for Life Sciences Partners, a biotech venture capital firm located in Amsterdam. All other authors declare that they have no competing interests. **Data and materials availability:** All data needed to evaluate the conclusions in the paper are present in the paper and/or the Supplementary Materials. R-spondin1–producing cells are available from C. Kuo under a material transfer agreement with Stanford University. Wnt3a- and Noggin-producing cells are available from H.C. under a material transfer agreement with the Hubrecht Institute. Distribution of PDOs and deposition of DNA sequencing data in publicly available databases are regulated by the informed consent that participants to this study signed. PDOs, clinical outcome, DNA sequencing data, and safety data on a per-patient level can be obtained through the Institutional Review Board of the Netherlands Cancer Institute (IRB@nki.nl). All other codes and materials used in this study are freely or commercially available.

Submitted 3 June 2019
Accepted 17 September 2019
Published 9 October 2019
10.1126/scitranslmed.aay2574

Citation: S. N. Ooft, F. Weeber, K. K. Dijkstra, C. M. McLean, S. Kaing, E. van Werkhoven, L. Schipper, L. Hoes, D. J. Vis, J. van de Haar, W. Prevoo, P. Snaebjornsson, D. van der Velden, M. Klein, M. Chalabi, H. Boot, M. van Leerdam, H. J. Bloemendal, L. V. Beerepoot, L. Wessels, E. Cuppen, H. Clevers, E. E. Voest, Patient-derived organoids can predict response to chemotherapy in metastatic colorectal cancer patients. *Sci. Transl. Med.* **11**, eaay2574 (2019).

Downloaded from http://stm.sciencemag.org/ by guest on July 22, 2021

Science Translational Medicine

Patient-derived organoids can predict response to chemotherapy in metastatic colorectal cancer patients

Salo N. Ooft, Fleur Weeber, Krijn K. Dijkstra, Chelsea M. McLean, Sovann Kaing, Erik van Werkhoven, Luuk Schipper, Louisa Hoes, Daniel J. Vis, Joris van de Haar, Warner Prevoo, Petur Snaebjornsson, Daphne van der Velden, Michelle Klein, Myriam Chalabi, Henk Boot, Monique van Leerdam, Haiko J. Bloemendal, Laurens V. Beerepoot, Lodewyk Wessels, Edwin Cuppen, Hans Clevers and Emile E. Voest

Sci Transl Med **11**, eaay2574.
DOI: 10.1126/scitranslmed.aay2574

Dishing out treatment recommendations

The number of treatment options for cancer patients keeps expanding, but it remains difficult to predict which tumors will be sensitive to which treatments. As a result, most patients receive treatment according to standardized protocols. With this approach, some patients respond to treatment, but others only experience side effects. To help address this situation, Ooft *et al.* developed a method of testing drugs in patient-derived organoids, biopsy-derived cells from individual patients grown in a dish. In a clinical study, the responses of organoids to irinotecan correlated with patients' responses to the drug, suggesting that organoids could help avoid giving irinotecan to patients who would not benefit.

ARTICLE TOOLS http://stm.sciencemag.org/content/11/513/eaay2574

SUPPLEMENTARY MATERIALS http://stm.sciencemag.org/content/suppl/2019/10/07/11.513.eaay2574.DC1

RELATED CONTENT
http://stm.sciencemag.org/content/scitransmed/8/344/344ra84.full
http://stm.sciencemag.org/content/scitransmed/11/478/eaau5758.full
http://stm.sciencemag.org/content/scitransmed/9/386/eaag2513.full
http://stm.sciencemag.org/content/scitransmed/10/427/eaam7610.full
http://stm.sciencemag.org/content/scitransmed/12/549/eaaz1723.full
http://stm.sciencemag.org/content/scitransmed/12/555/eaax8313.full
http://stm.sciencemag.org/content/scitransmed/13/603/eabf3637.full

REFERENCES This article cites 32 articles, 9 of which you can access for free
http://stm.sciencemag.org/content/11/513/eaay2574#BIBL

PERMISSIONS http://www.sciencemag.org/help/reprints-and-permissions

Use of this article is subject to the Terms of Service

Science Translational Medicine (ISSN 1946-6242) is published by the American Association for the Advancement of Science, 1200 New York Avenue NW, Washington, DC 20005. The title *Science Translational Medicine* is a registered trademark of AAAS.

Copyright © 2019 The Authors, some rights reserved; exclusive licensee American Association for the Advancement of Science. No claim to original U.S. Government Works

Downloaded from http://stm.sciencemag.org/ by guest on July 22, 2021